Dynamic running actions on footbridges: a pilot study on human-structure interaction

J. Lottefier & P. Van den Broeck & K. Van Nimmen
Department of Civil Engineering, Structural Mechanics
KU Leuven, B-3001 Leuven, Belgium

ABSTRACT: Running has become a popular leisure activity, evidenced by the increasing popularity of urban trails and marathons. However, assessment of the structural response induced by runners on civil engineering structures, such as footbridges and floors, is very challenging due to inadequate prediction models. The lack of fundamental data and qualitative research approaches obstruct the characterisation of Human-Structure Interaction (HSI). Specifically active HSI, when the human locomotion is influenced by the motion of the supporting surface, is not well understood. This contribution presents a pilot study on active HSI for dynamic running actions. The cycle-by-cycle gait parameters were captured using a state-of-the-art moveable treadmill setup. The proposed analysis method revealed only an impact of additional structural excitations on the peak force amplitudes but not on the body motion. The reduced force amplitudes are related to a possible decreased relative phase difference between the runner and the structure, and thus, an indication of active HSI.

1 INTRODUCTION

Economic incentives stimulate the use of new materials which are proportional much stronger and lighter compared to conventional construction materials. New composite materials are applied in footbridge design such as Fibre Reinforced Polymers (FRP). However, due to the limited structural mass, high slenderness and low inherent damping, modern civil engineering structures are at risk to exhibit excessive vibrations during their service (Živanović et al. 2017). For many footbridges, floors and grandstands, the Vibration Serviceability Assessment (VSA) has become the key design criterion. In addition, the currently available response prediction models are over-conservative, leading to unnecessary costs and retrofits (Ahmadi et al. 2019). To address the shortcomings, the load model(s) should account for the variability inherent in human gait and the influence of the interaction between the structure and the users, denoted as Human-Structure Interaction (HSI). Mechanical interaction between the structure and the human body, acting as a spring mass damper, results in a coupled system with increased mass and damping (Van Nimmen et al. 2017), called passive HSI (pHSI).

Moreover, humans are sensitive to different external stimuli and consciously or subconsciously adapt the body motion to the environment (Mohammed and Pavic 2021). Structural vibrations can be such a stimulus, as for example, the lock-in phenomenon demonstrated in lateral vibrations (Živanović et al. 2005). In parallel, vibrations in the vertical direction have been studied and have shown to increase the variability of the pacing rate for increasing levels of vertical excitation during walking (Dang and Živanović 2016, Ahmadi et al. 2018). Moreover, both studies also confirmed a statistically significant drop in the magnitude of the walking force harmonic closest to the vibration frequency. The phenomenon where the human locomotion is influenced by the motion of the supporting surface is denoted as active HSI (aHSI).

The type of loading has a decisive impact on the resulting structural response. Running is characterised by a higher dominant frequency spectrum (pacing rate) and higher load amplitudes compared to the walking excitation. In contrast to walking, where HSI has been well investigated, the effects of HSI during running are not well understood. To the best of the author's knowledge, only a very limited number of studies investigate the load case running for civil engineering practice. In this paper, a first draft of a measurement setup involving one person running on a rigid and vibrating surface is presented. In this way, a first preliminary assessment of the potential influence of aHSI is made. The effects of pHSI are for the proposed experiments (solo running) negligible because the mass ratio between one person and a civil structure is extremely small.

After this introduction, the laboratory and in situ measurements are described and followed by a discussion of the results and some preliminary conclusions. The paper concludes by revisiting the potential and limitations of the considered experimental setup, and makes suggestions for further research.

2 MEASUREMENT CAMPAIGN

If human locomotion is influenced and altered by the motion of the supporting surface, then the measured locomotion on a flexible surface (footbridge) should be statistically different from that on a rigid surface (laboratory). To investigate aHSI, a measurement campaign was performed on both surfaces. Measurements on a rigid surface were conducted at the Structural Mechanics research laboratory in Ghent to serve as a reference dataset. The Eeklo footbridge was selected for the measurements on a vibrating surface.

It is expected that the change of the gait cycle is related to the amplitude and frequency of the structural vibrations. To allow for a range of vibration amplitudes, the original idea was to place the measurement setup on different locations on the bridge deck. In this way, different acceleration levels are to be expected. However, during the measurement campaign only one location was used, for details see section 2.4. An additional test protocol was designed involving three persons bobbing at midspan to further increase the vibration amplitude. The vibration frequency was controlled by guiding the test subjects to run at the resonance frequency of a vertical bending mode of the Eeklo footbridge (2.99 Hz; see section 2.2).

Thus, three different test protocols are presented in this paper: solo running at 2.99 Hz (1) under laboratory conditions, (2) on the Eeklo footbridge and (3) on the Eeklo footbridge with additional excitation of the bridge deck (by bobbing).

2.1 *Test subjects*

A total of four Test Subjects (TSs) (3 males and 1 female with age and body mass respectively ranging from 31 to 52 years and 53 to 90 kg) were involved in the measurement campaign, see Table 1. All volunteers were drawn from the population of students and academics of KU Leuven at Technology Campus Ghent. Every TS was asked to run at a self-selected speed at which they could run comfortably at the imposed step frequency of 2.99 Hz, guided by a metronome. Due to practical limitations, TS 1 only took part in the tests performed on the Eeklo footbridge (no reference measurement).

2.2 *Description of the Eeklo footbridge*

The footbridge considered in these measurements is located in Eeklo, Ghent and is frequently used by cyclist, joggers and pedestrians to cross the N49 road (Van Nimmen et al. 2014). The footbridge consists of one main (arc-shaped) and two side (straight) beams with a total span of 96 meters and a total width of 3 meter (Van Hauwermeiren et al. 2020). A more comprehensive and detailed description of the footbridge can be found in (Van Nimmen et al. 2014). The mode shape of interest in this paper is the first vertical bending mode characterized by a natural frequency of 2.99 Hz, a damping ratio of 0.2% and a modal mass of 22×10^3 kg. A pacing rate of 2.99 Hz is in the fast running range according to (Occhiuzzi et al. 2008). The theoretical response of one perfectly periodic person running at the resonance frequency was calculated at midspan (location with maximal modal displacement). The half sine load model (Bachmann and Ammann 1987) was used with an impact factor k_p equal to 2.5 while the body mass was set to 700 N. The theoretical steady state response at midspan is estimated at 9.61 m/s^2. Additional locations were considered to obtain a steady state response of respectively 25%, 50% and 75% of the steady state response at midspan. In this way, the influence of the vibration amplitude on aHSI can be observed. The other locations are respectively at a distance of 34.8m, 38.3m and 41.4m from the bridge ends with midspan at 48m.

2.3 *Moveable treadmill setup*

A database, specifically developed to observe the effects of aHSI, was collected using a predefined test protocol. To this end, a state-of-the-art moveable treadmill setup is used which allows the detection of the 3D body motion and other relevant running motion metrics on a cycle-by-cycle basis, see Figure 1. The measurement setup consists of (1) a movable treadmill, (2) an optical movement analysis system and a runner equipped with (3) inertial motion trackers and (4) insole pressure sensors.

A treadmill (Lode Valliant 2 Rehab, Netherlands) is used in order to reach the steady state response which is not easily reached in the time window of one crossing, especially for short footbridges. Moreover, a treadmill ensures a constant (self-selected) speed. The optical movement analysis system (OPTOGait, Microgate S.r.I, Italy, 2010), or optical sensor, is mounted rigidly to the treadmill by touch fasteners. This photoelectric cell system can determine spatiotemporal gait parameters through the interruptions in the infrared communication between one transmitting and one receiving LED bar (Microgate S.r.l. 2012). Additionally, an inertial motion tracker (GYKO REPOWER, Microgate S.r.I, Italy, 2015) is connected via software to the optical sensor through a Bluetooth connection. Therefore, the device is further denoted as the Bluetooth accelerometer. A second inertial motion sensor (X16-1D USB accelerometer, Gulf Coast Data Concepts, USA) is used as a redundant measure, denoted as the USB accelerometer.

Table 1: Age, anthropometric characteristics and running speed per test subject.

Subject ID	Age [year]	Mass [kg]	Leg Length inside [m]	Leg Length outside [m]	Running speed [km/h]
1	34	53	0.69	0.86	7.5
2	31	90	0.86	1	9.9
3	31	73	0.74	0.93	11.5
4	52	80	0.74	0.93	10.5

Insole pressure units (Pedar-X, NovelGmbH, Munich, Germany) capture the plantar pressure distribution in time. In contrast to more conventional pressure measuring devices, such as force plates or an instrumented treadmill, an insole measurement is not spatially limited. Thus, they have shown to be a convenient technology to measure the Ground Reaction Forces (GRFs) for in situ applications (Hsiao et al. 2002, Koch et al. 2016, Price et al. 2016). One of the limitations of insole pressure sensors is that they measure pressure and the normal force, perpendicular to the sensor, which does not represent the vertical GRF during the initial and late stance phase of the gait cycle (Barnett et al. 2001, Stöggl and Martiner 2017).

The structural accelerations were recorded with a data-acquisition system of National Instruments consisting of 2 NI 9234 4-Channel Sound and Vibration Input Modules in a NI cDAQ-9178 CompactDAQ Chassis.

Figure 1: The state-of-the-art moveable treadmill setup.

2.4 *Test protocol*

Each test involves just one TS active on the treadmill. First, the TS was equipped with the insoles pressure units and two inertial motion sensors. Consecutively, anthropometric data were measured (see Table 1) and the participant took place on the treadmill. To ensure resonance with the footbridge, a metronome was used. The self-selected speed (determined during a preliminary test in the laboratory, see Table 1) was kept constant during each test involving the same TS. The total test duration was set to 5 min.

To observe the effect of aHSI at different vibration amplitudes, the initial plan was to place the measurement setup at four different locations corresponding to 25%, 50%, 75% and 100% of the steady state response at midspan. However, as can be seen on Figure 2 in section 3.2, when the setup was placed at midspan, the structural response was much lower than theoretically estimated (maximum response for TS 1 is 1.5 m/s²). Therefore, all tests on the Eeklo footbridge were performed at midspan.

To further increase the structural response, to allow the analysis of aHSI for higher structural acceleration levels, additional external excitation of the structure was obtained by bobbing of three people. In this way, two different test protocols were used on the Eeklo footbridge: (1) without and (2) with additional excitation. In this latter case, three volunteers were bobbing at the resonance frequency of 2.99 Hz and were placed randomly on the bridge deck in the proximity of one meter of the measurement setup. The bobbing frequency was guided by a metronome which was hearable for everyone involved (amplified by a wireless sound system).

Due to practical considerations and to allow free passage on the structure, the treadmill setup was placed close to one of the side beams of the footbridge, which had a minor influence on the steady state response (theoretical decrease of 0.24 m/s²).

2.5 *Data collection and acquisition*

A wireless connection was established with the Bluetooth accelerometer and the insole pressure units through two Bluetooth dongles inserted in the data acquisition computer. In contrast, the optical sensor was directly wired to the computer (USB A+B cable). The USB accelerometer operated independently while the structural response data-acquisition system was connected to a second independent acquisition computer.

The OptoGait software (OptoGait version 1.12.19.0) combines the measured discrete data of the Bluetooth accelerometer with the optical sensor data and sets the data acquisition parameters as recommended by the manufacturer, assessed in (Healy et al. 2019).

All data is saved in a format that is suitable for later analysis in MATLAB. Per trial, the spatiotemporal parameters and acceleration signals are exported into an XML file while the force data is saved in TXT files and Novel software specific file formats and the structural response as binary MATLAB files. USB accelerometer data is saved locally on the device as a CSV file. The sampling frequency is respectively

2048 Hz, 1000 Hz, 500 Hz, 200 Hz and 100 Hz for the structural response, the optical sensor, the Bluetooth accelerometer, the USB accelerometer and the insole pressure units.

Due to the malfunction of the USB accelerometer, the structural response could not accurately be synchronized with the 3D body motion. Additionally, it is assumed that both the insole pressure units and the Bluetooth accelerometer start at the same time instant. Consequently, the synchronization between the structural response, the 3D body motion and the insole pressure units is rather poor.

3 RESULTS

3.1 *Experimental data pre-processing*

Vector projection is used to orientate the signals into the vertical direction by applying the properties of the gravitational acceleration vector. Every time signal is resampled, to ensure a constant time step of 0.005 sec, and filtered by applying at fifth order Butterworth band-pass filter between 0.5 and 20 Hz, except for the vertical force-time data which is filtered by applying a fifth order Butterworth low-pass filter with a cut off frequency of 20 Hz.

Since the runner has to first gain speed and accommodate to the treadmill at the start of the test (White, Gilchrist, & Christina 2002), only a predefined window of the data is used in the analysis of aHSI. Moreover, the tests are designed to run at a nearly constant structural vibration amplitude. Therefore, the relevant start is chosen when in the theoretical case the footbridge reached approximately 96% of the steady state response (when only the resonance mode is considered). The relevant time window was set between 90 sec and 5 min after the start of the test.

When analysing the body motion and the GRFs, both the absolute peak amplitudes and the peak amplitudes of the first harmonic (fundamental) are considered. These latter amplitudes are in resonance with the structure and therefore key in analysing aHSI. To this end, first the Power Spectral Density (PSD) is calculated, via Welch's method with a Gaussian window with a length of 15sec and 50% overlap, from which the fundamental harmonic frequency is identified. Secondly, the signals are filtered around the first harmonic, by a fifth order Butterworth band-pass filter between [0.5 - 1.5] times the fundamental harmonic frequency. Based on the technique proposed in (Van Nimmen et al. 2014) the Time Variant Pacing Rate (TVPR) is derived from the signals filtered around the first harmonic component. The term TVPR corresponds to a distribution of pacing rates defined as the inverse of the time spacing between two peaks in the acceleration or force signal, filtered around the first harmonic. Each calculated pacing rate is associated to the time instant of the second peak.

The results are checked for normality by means of a normalized chi-squared test. The norm difference between the normalized histogram and the normal probability density function, according to the data, is divided by the norm of the normal distribution. In this way, a percentage for normality of the data is found.

3.2 *Structural response*

Simulations performed in MATLAB estimated a steady state response equal to 9.61 m/s^2 at midspan. The measured vibration amplitude is much lower than predicted, even with additional excitation as is the case for TP 1 with a maximum at 4 m/s^2, and is characterized by many fluctuations, Figure 2. The average response is at least 75% lower in all trials.

On the one hand, intra-subject variability, that is the difference between consequent steps performed by the same person (Racic, Pavic, & Brownjohn 2009), cause such a non-stationary structural response. Monte Carlo simulations (100 performed) revealed only a drop of 1.5 m/s^2 in both the mean and maximum structural response when the pacing rate follows a normal distribution around 2.99 Hz with a standard deviation of 0.11 Hz. On the other hand, when analysing the structural response of each trial in the frequency spectrum, the fundamental frequency is always lower than 2.99 Hz with a lowest measured natural frequency of 2.96 Hz. A theoretical change of the natural frequency to 2.96 Hz when running perfectly periodic at 2.99 Hz indicates a reduction of 80% of the vibration amplitude after 90sec. The reduction of the natural frequency is explained by the added mass of the treadmill (249 kg) on the structure.

Thus, due to the frequency mismatch, the runner is near-resonant with the structure. In this situation, the runner is at one point in resonance with the structure, due to intra-variability, but forced to lose resonance due to the metronome beat, resulting in a non stationary response. The combined effect of a lower natural frequency and intra-variability clarifies the low measured structural response, whereby the changed modal characteristic has the most distinct effect.

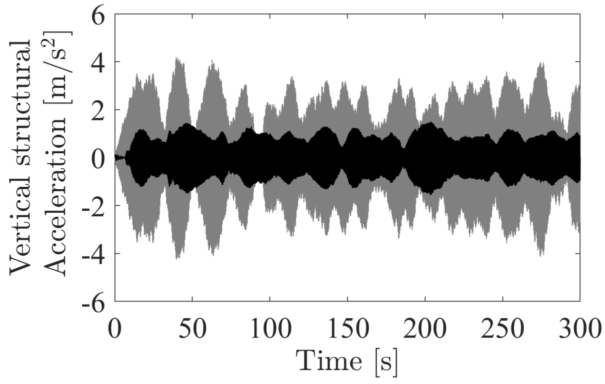

Figure 2: The structural accelerations in vertical direction for test subject 1 during solo running on the Eeklo footbridge at 2.99 Hz; without (black) and with (grey) additional excitation.

3.3 *Amplitude body motion*

Body motion amplitudes are detected by the Bluetooth accelerometer, see section 3.1. The error plot, indicating the numerical mean minus and plus one time the standard deviation, for the three considered test protocols. Both the total and the fundamental harmonic amplitude of the vertical body motion are presented Figure 3. The mean and standard deviation of TS 4 stand out as the largest.

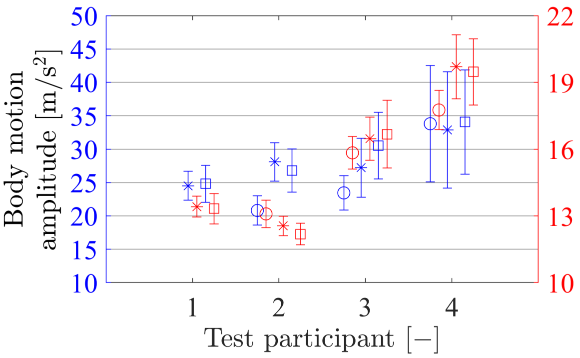

Figure 3: Error plot of body motion in terms of the total (blue) and fundamental (red) amplitude per test subject and per test protocol; on rigid surface (○) and on the Eeklo footbridge without (∗) and with (□) additional excitation.

The distribution of the body motion amplitude is related to a normal distribution, see Figure 4. For the total amplitude, the normality fit is between 65% and 84% for TS 1, 2 and 3 across the different tests. However, for TS 4, the normality fit is very poor, between 1% and 15%. For the fundamental harmonic amplitude, see Figure 4 in red, the same conclusion is drawn, the normality fit is between 66% and 86% for participant 1,2 and 3, and between 34% and 56% for TS 4.

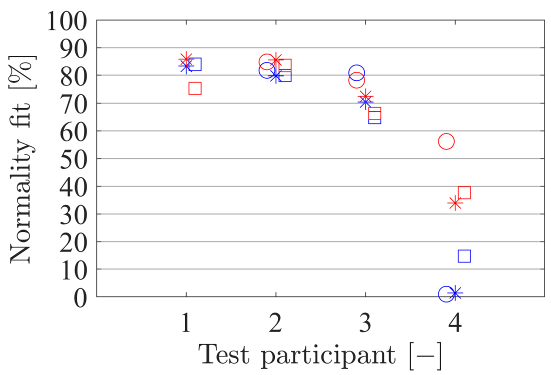

Figure 4: Chi-squared normality fit for the total (blue) and fundamental (red) body motion ampltiude per test protocol; on rigid surface (○) and on the Eeklo footbridge without (∗) and with (□) additional excitation.

When analysing the fundamental body motion amplitude for TS 4, it is observed in Figure 5 that the values are distributed around two separate means. Therefore, a distinction between the left and right foot is made. The normality fit, re-calculated per foot, increased to minimum 70% and 63% for respectively the total and fundamental body motion amplitude. TS 4 clearly has an asymmetric gait cycle.

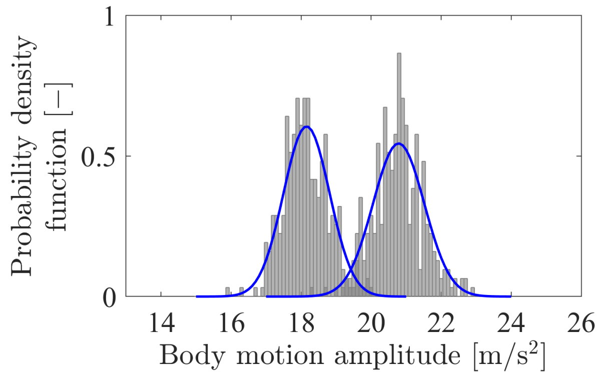

Figure 5: The distribution of the fundamental body motion amplitudes with a distinction between the two feet for test subject 4 on the Eeklo footbridge with additional excitation.

3.4 *Peak force amplitude*

The peak force amplitude, or impact factor k_p in the half sine model, is the peak force measured by the insole pressure units divided by the body mass, shown together with the fundamental component in Figure 6. One could notice that the peak force amplitude across all TSs is consistently lower for a trail with additional excitation of the bridge compared to a trail without.

The normality test is high for almost all considered tests with a normality fit between 66% and 94% and between 86% and 97% for respectively the impact factor and the fundamental peak force amplitude (the resonance force harmonic with the structure). However, for TS 2 during the trial with additional excitation, the normality test is much lower with respectively 29% and 45% for the impact factor and the fundamental peak force amplitude.

Interestingly, no asymmetry between the left and right foot for TS 4 is observed in the peak force amplitude. This has a potential physiological explanation where each leg has a different damping ratio. Consequently, the same induced force is damped differently which results in an asymmetric motion of the trunk.

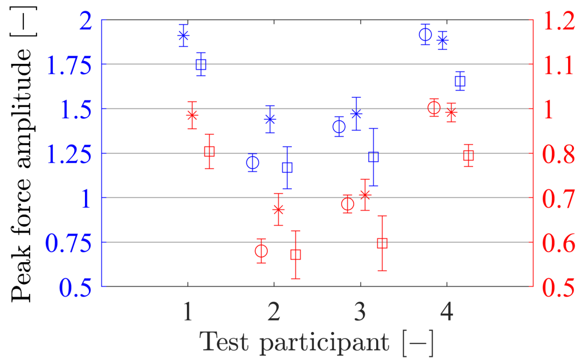

Figure 6: Error plot of peak force amplitude in terms of the total (blue) and fundamental (red) per test subject and per test protocol; on rigid surface (○) and on the Eeklo footbridge without (∗) and with (□) additional excitation.

3.5 *The Time Variant Pacing Rate*

The TVPR is measured by the optical sensor, the Bluetooth accelerometer, the USB accelerometer and the insole pressure sensors, Figure 7 for errorplot. Good agreement between the insole pressure sensors and the Bluetooth accelerometer is found in terms of the average pacing rate ($t - test$ lowest p-value of 0.79 for TS4 on rigid surface) but not for the standard deviation ($F - test$ reject null hypothesis for TS 2 and 4 on rigid surface at 5% significance level). On rigid surface, the USB accelerometer also shows similar agreement ($t - test$ lowest p-value of 0.87 for TS3 while $F - test$ reject null hypothesis for TS 3 and 4 at 5% significance level). In contrast, in most cases, the optical sensor gives a much larger standard deviation, with a comparable average value. For TS 2, an unrealistic distribution is found for all considered tests and are therefore excluded. During the tests it was noticed that participant 2 had a walking-like gait cycle, which is reflected in the low speed of travel compared to TSs with a similar height, see Table 1. This may also explain the low normality fit for the peak force amplitudes (see section 3.4).

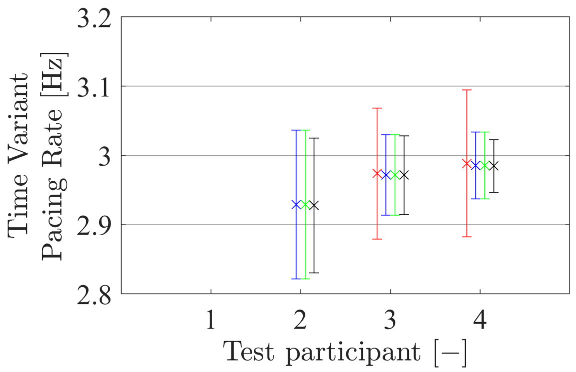

Figure 7: Error plot of Time Variant Pacing Rate per test subject for trials on a rigid surface measured by the optical sensor (red), the Bluetooth accelerometer (blue), the USB accelerometer (green) and the insole pressure units (black).

The normality test for the TVPR is high in all cases, with a minimum normality fit of 66%. In the rest of the paper, the data obtained from the Bluetooth accelerometer will be used to characterize the influence of the vibrating surface on the TVPR.

4 ANALYSIS OF ACTIVE HUMAN-STRUCTURE INTERACTION

4.1 *Analysis method*

In this section, the running gait is studied on a cycle-by-cycle basis in function of the structural response at each time instant. For this analysis, the body motion and the GRFs are investigated and are related to the peak structural response at each time instant during the trial. Note that the TVPR is associated with the time instant of the second peak. For each structural response peak value, a relative time window of one half of the average pacing period before and after this peak is considered. Each body motion amplitude, pacing rate, peak force amplitude and corresponding fundamental harmonic component within this window is associated to this peak response value. In this way, the parameters can be divided into vibration amplitude intervals. Per interval, the mean value is calculated. The analysis described here uses 20 acceleration intervals ranging from 0 to 5m/s² with a constant step of 0.25m/s². Due to the low number of samples in the lowest and highest acceleration intervals, it should be noted that the figures in the next subsections experience edge effects (fluctuations at the beginning and/or end).

4.2 *Analysis of the Time Variant Pacing Rate*

Figure 8 shows the TVPR across the vibration amplitude intervals for all trials on the Eeklo footbridge. The results for TS 1, 2 and 4 show a close overlap meaning the results of the tests on the Eeklo footbridge without and with additional excitation can be combined. For TS 3, this overlap is absent, which is most likely due to the inexperience the subject had with treadmill running. No clear trend can yet be identified to indicate that aHSI has an effect on the pacing rate when the results are combined per TS, presented in Figure 9.

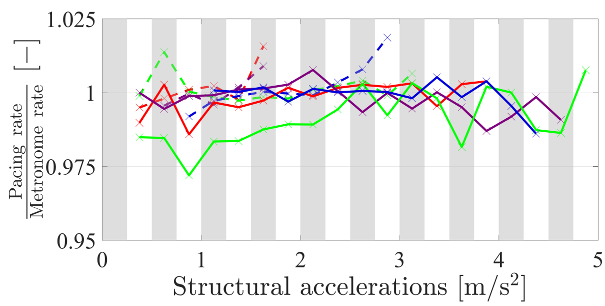

Figure 8: Normalized average Time Variant Pacing Rate per vibration amplitude interval for trials without (dashed line) and with (solid line) additional excitation and per Test Subject (TS); TS 1 (red), 2 (purple), 3 (green) and 4 (blue).

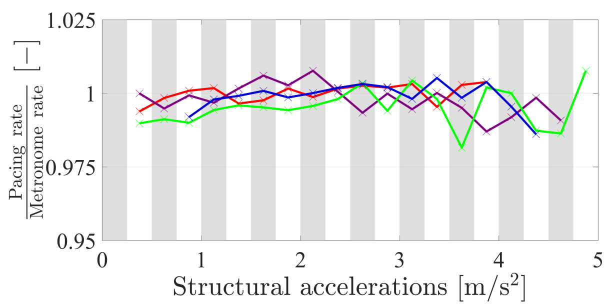

Figure 9: Normalized average Time Variant Pacing Rate per vibration amplitude interval per Test Subject (TS); TS 1 (red), 2 (purple), 3 (green) and 4 (blue).

4.3 *Analysis of the body motion amplitude*

The fundamental body motion amplitudes, see Figure 10, mostly overlap, and thus, are combined per TS in Figure 11. For TS 1, 2 and 4, a small decrease of body motion amplitude can be identified for higher structural acceleration levels. However, the opposite is true for TS 3. Given the small number of TSs, no clear conclusions can be drawn on the effect of aHSI on the body motion amplitude during running.

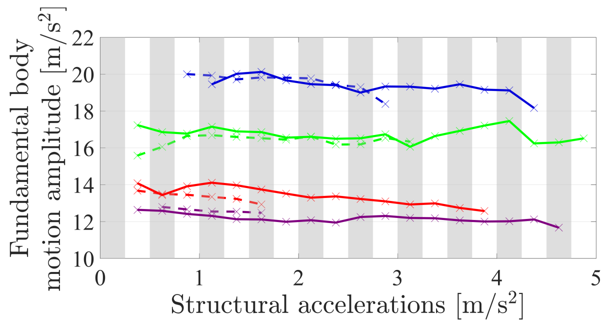

Figure 10: Average fundamental body motion amplitude per vibration amplitude interval for trials without (dashed line) and with (solid line) additional excitation and per Test Subject (TS); TS 1 (red), 2 (purple), 3 (green) and 4 (blue).

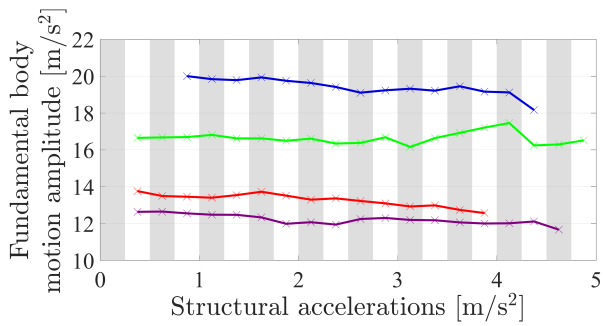

Figure 11: Average fundamental body motion amplitude per vibration amplitude interval per Test Subject (TS); TS 1 (red), 2 (purple), 3 (green) and 4 (blue).

4.4 *Analysis of the peak force amplitude*

In case no additional excitations are considered, the fundamental peak force amplitude, for the same vibration interval, is significant higher for every TS compared to the situation with bobbing as apparent from Figure 12. Therefore, the data per TS cannot be combined.

External excitation of the footbridge has the effect to decrease the propulsive input of one solo runner. In this way, the propulsive input of the TS is complemented with the propulsive input of the three bobbers, meaning the TS has to contribute less to the structural acceleration. A general decrease of the induced forces is observed for increasing structural acceleration levels. Lower propulsive forces are closely related to the relative phase difference between the runner and the structure. In biomechanics, it is known that the surface affects the running economy (metabolic rate)

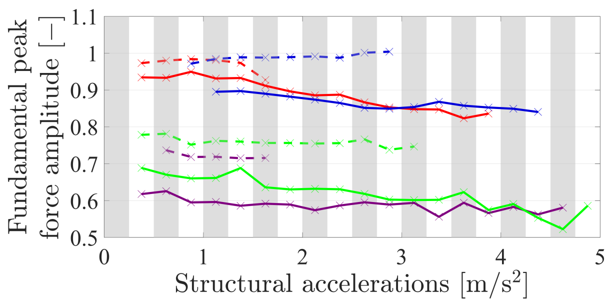

Figure 12: Average fundamental peak force amplitude per vibration amplitude interval for trials without (dashed line) and with (solid line) additional excitation and per Test Subject (TS); TS 1 (red), 2 (purple), 3 (green) and 4 (blue).

without affecting the running body motion (Kerdok et al. 2002). Humans tend to adjust their leg stiffness to accommodate changes in surface stiffness and to maintain a consistent gait style (Ferris et al. 1998). The total stiffness of the system, which consists of the runner and the surface, remains in this way constant. An increase in the surface stiffness results in higher peak GRFs but relatively also a higher leg compression. As a result, the leg stiffness decreases for a higher surface stiffness and higher forces are induced on the surface (Farley et al. 1998).

Due to dynamics, the footbridge surface acts as a surface with changeable stiffness. When the propulsive force induced by the runner is high, the footbridge acts as a very stiff surface, indicating the bridge deck is working against the runner's feet or in counterphase and the leg stiffness is low. Similarly, when the propulsive force is low, as during bobbing conditions, the footbridge acts as a soft surface and thus, more in phase with the body motion. This effect seems larger for higher structural acceleration levels. Note that this mechanical property predicts no considerable change in the body motion amplitude or pacing rate (for the same structural acceleration levels) as has been found in section 4.2 and section 4.3.

5 CONCLUSION

No clear differences are observed between the trials on the Eeklo footbridge at the same structural accelerations for the body motion amplitude and the TVPR and, thus, additional excitation of the structure does not influence the locomotion at the level of the Body Centre Of Mass (BCOM), in terms of amplitude and pacing rate. Therefore, the results of both test are combined and analysed together against the structural vibration level. No clear trend can be concluded, further research involving more TSs is required. Although, one could already indicate that aHSI may not affect the TVPR and the body motion amplitude during such measurement conditions, i.e. forced resonance treadmill running. In contrast, the peak force amplitudes clearly show a difference between the trials on the Eeklo footbridge. For the trials with additional excitation, the peak force amplitude is lower for all TSs. A lower propulsive force is related to an increased leg stiffness and a decreased surface stiffness. This latter is explained by a smaller relative phase difference between the structure and the human body motion and, thus, an indication of aHSI.

6 FURTHER RECOMMENDATIONS

The proposed state-of-the-art moveable treadmill setup showed its capability to reliably capture the human body motion and GRFs in a relative straightforward manner. Although some preliminary conclusions have been drawn, further research is needed. New plans have been formulated to investigate aHSI using modified test protocols. To this end, a mechanical shaker will be used to insure a stationary response, even before the TS starts to run. In this way, the TS can run at a self-selected speed and pacing rate, no metronome needed, and different vibration amplitudes can be applied and closely monitored. Furthermore, more TSs will be involved in the next measurement campaign.

The most important aspect that is currently missing in this paper is the relative phase information between the structure, the body motion and the GRFs. Therefore, a synchronization approach has been developed to synchronize the measurement devices precisely in future measurements.

7 ACKNOWLEDGEMENTS

This research is funded by the Research Foundation Flanders (FWO). The financial support is gratefully acknowledged. The author would also like to thank Benedicte Vanwanseele for her support during the interpretation of the measurement results and development of the modified test protocols.

REFERENCES

Ahmadi, E., C. Caprani, S. Živanović, & A. Heidarpour (2019). Assessment of human-structure interaction on a lively lightweight GFRP footbridge. *Engineering Structures 199*, 109687.

Ahmadi, E., C. Caprani, S. Živanović, & A. Heidarpour (2018). Vertical ground reaction forces on rigid and vibrating surfaces for vibration serviceability assessment of structures. *Engineering Structures 172*, 723–738.

Bachmann, H. & W. Ammann (1987). *Vibrations in structures: induced by man and machines*, Volume 3. Iabse.

Barnett, S., J. L. Cunningham, & S. West (2001). A comparison of vertical force and temporal parameters produced by an in-shoe pressure measuring system and a force platform. *Clinical Biomechanics 16*(4), 353–357.

Dang, H. V. & S. Živanović (2016). Influence of low-frequency vertical vibration on walking locomotion. *Journal of Structural Engineering 142*(12), 04016120.

Farley, C. T., H. H. Houdijk, C. Van Strien, & M. Louie (1998). Mechanism of leg stiffness adjustment for hopping on surfaces of different stiffnesses. *Journal of applied physiology 85*(3), 1044–1055.

Ferris, D. P., M. Louie, & C. T. Farley (1998). Running in the real world: adjusting leg stiffness for different surfaces. *Proceedings of the Royal Society of London. Series B: Biological Sciences 265*(1400), 989–994.

Healy, A., K. Linyard-Tough, & N. Chockalingam (2019). Agreement between the spatiotemporal gait parameters of healthy adults from the optogait system and a traditional three-dimensional motion capture system. *Journal of biomechanical engineering 141*(1), 014501.

Hsiao, H., J. Guan, & M. Weatherly (2002). Accuracy and precision of two in-shoe pressure measurement systems. *Ergonomics 45*(8), 537–555.

Živanović, S., A. Pavic, & P. Reynolds (2005). Human–structure dynamic interaction in footbridges.

Živanović, S., X. Wei, J. W. Russell, & J. T. Mottram (2017). Vibration performance of two FRP footbridge structures in the United Kingdom.

Kerdok, A. E., A. A. Biewener, T. A. McMahon, P. G. Weyand, & H. M. Herr (2002). Energetics and mechanics of human running on surfaces of different stiffnesses. *Journal of applied physiology*.

Koch, M., L.-K. Lunde, M. Ernst, S. Knardahl, & K. B. Veiersted (2016). Validity and reliability of pressure-measurement insoles for vertical ground reaction force assessment in field situations. *Applied ergonomics 53*, 44–51.

Microgate S.r.l. (2012). *User Manual Optogait*. Micrgate S.r.l.

Mohammed, A. & A. Pavic (2021). Human-structure dynamic interaction between building floors and walking occupants in vertical direction. *Mechanical Systems and Signal Processing 147*, 107036.

Occhiuzzi, A., M. Spizzuoco, & F. Ricciardelli (2008). Loading models and response control of footbridges excited by running pedestrians. *Structural Control and Health Monitoring: The Official Journal of the International Association for Structural Control and Monitoring and of the European Association for the Control of Structures 15*(3), 349–368.

Pavic, A., M. Willford, P. Reynolds, & J. Wright (2002). Key results of modal testing of the Millennium Bridge, London. *Proceedings of Footbridge*.

Price, C., D. Parker, & C. Nester (2016). Validity and repeatability of three in-shoe pressure measurement systems. *Gait & posture 46*, 69–74.

Racic, V., A. Pavic, & J. Brownjohn (2009). Experimental identification and analytical modelling of human walking forces: Literature review. *Journal of Sound and Vibration 326*(1-2), 1–49.

Stöggl, T. & A. Martiner (2017). Validation of moticon's opengo sensor insoles during gait, jumps, balance and cross-country skiing specific imitation movements. *Journal of sports sciences 35*(2), 196–206.

Van Hauwermeiren, J., K. Van Nimmen, P. Van den Broeck, & M. Vergauwen (2020). Vision-based methodology for characterizing the flow of a high-density crowd on footbridges: Strategy and application. *Infrastructures 5*(6), 51.

Van Nimmen, K., G. Lombaert, G. De Roeck, & P. Van den Broeck (2017). The impact of vertical human-structure interaction on the response of footbridges to pedestrian excitation. *Journal of Sound and Vibration 402*, 104–121.

Van Nimmen, K., G. Lombaert, I. Jonkers, G. De Roeck, & P. Van den Broeck (2014). Characterisation of walking loads by 3D inertial motion tracking. *Journal of Sound and Vibration 333*(20), 5212–5226.

White, S. C., L. A. Gilchrist, & K. A. Christina (2002). Within-day accommodation effects on vertical reaction forces for treadmill running. *Journal of Applied Biomechanics 18*(1), 74–82.